Microscopy and Microanalysis, **29** (Suppl 1), 2023, 1626–1627
https://doi.org/10.1093/micmic/ozad067.835

Microscopy AND Microanalysis

Meeting-report

Visualizing Polar Distortions and Interface Effects with Multislice Ptychography

K.P. Harikrishnan[1], Yilin Evan Li2, Kevin J. Crust[3,4], Aarushi Khandelwal[3,5], Yu-Tsun Shao[1,6], Zhen Chen[7], Chenyu Zhang[1], Christo Guguschev[8], Ruijuan Xu[3,5,9], Harold Y. Hwang[3,5], Darrell G. Schlom[2,8,10], and David A. Muller[1,10,*]

[1]*School of Applied and Engineering Physics, Cornell University, Ithaca, NY, United States*
[2]*Department of Materials Science and Engineering, Cornell University, Ithaca, NY, United States*
[3]*Stanford Institute for Materials and Energy Sciences, SLAC National Accelerator Laboratory, Menlo Park, CA, United States*
[4]*Department of Physics, Stanford University, Stanford, CA, United States*
[5]*Department of Applied Physics, Stanford University, Stanford, CA, United States*
[6]*Mork Family Department of Chemical Engineering and Materials Science, University of Southern California, Los Angeles, CA, United States*
[7]*School of Materials Science and Engineering, Tsinghua University, Beijing, China*
[8]*Leibniz-Institut für Kristallzüchtung, Berlin, Germany*
[9]*Department of Materials Science and Engineering, North Carolina State University, Raleigh, NC, United States*
[10]*Kavli Institute at Cornell for Nanoscale Science, Ithaca, NY, United States*

*Corresponding author: david.a.muller@cornell.edu

Exotic properties associated with the emerging class of quantum materials are often coupled to picometer-scale lattice modulations in the host material. Although scanning transmission electron microscopy (STEM) is one of the foremost techniques for such atomic-scale characterization, conventional STEM imaging modalities are prone to artifacts arising from channeling effects, crystal mistilts and surface relaxations. Annular bright field (ABF) and differential phase contrast (DPC) techniques have well-documented errors arising from variations in the diffraction condition [1, 2]. High-angle annular dark field (HAADF) imaging, although often more tolerant to diffraction artifacts, fails to capture the rich information encoded in the atomic positions of lighter atoms.

With recent improvements in direct electron detectors [3, 4], electron ptychography has enabled reconstructions of the electrostatic scattering potential [5] and mapping of electromagnetic fields [6] at resolutions beyond the diffraction limit. Multislice ptychography incorporates the multislice algorithm with the phase-retrieval algorithm and offers a potentially robust method for resolving the structure [7] in thick samples (~30 nm). By modeling the full scattering physics, the technique solves the multiple-scattering problem and accounts for any channeling of the electron beam in crystalline samples. Moreover, post processing of the reconstructions can remove any effects from crystal mistilts or surface relaxation in the sample. The capability of the technique for thermal-vibration-limited lateral resolution, depth sectioning and light-atom imaging has enabled direct visualization of structural features that are currently beyond the reach of any other technique and is illustrated using two examples here.

Figures 1(a) and (b) show a direct comparison between HAADF and ptychography images of Mg, Zr-doped strontium hexagallate ($SrGa_{12}O_{19}$) [8] where the capability to image oxygen atoms and enhanced lateral resolution in the ptychographic reconstruction is evident. The material has an unstable phonon mode associated with the gallium atom in the trigonal bipyramidal site, which can displace up or down along the vertical c-axis to create a local polarization. Depth sectioning of the ptychographic reconstruction allows direct mapping of these polar distortions [9] and is illustrated in Fig. 1(c-f) which shows different slices in depth, of the region marked with a white box in (b). A depth profile corresponding to the yellow line in Fig. 1(b) is shown in (g), displaying the changing occupancy of the two bistable gallium sites as a function of depth.

For thin films, the interface structure can not only play a crucial role in the properties of the film, but also often host emergent properties. Figures 2(a) and (b) show the ptychographic reconstructions of the interface between ferroelectric $NaNbO_3$ (NNO) thin film synthesized by pulsed laser deposition and $DyScO_3$ (DSO) substrate along two orthogonal directions. The high-resolution imaging of the interface allows for precise measurements of the variations in bond length, bond angles, etc. which can critically affect the energy balance between different kinds of polar and magnetic ordering in perovskite structures. Along the $[1\bar{1}0]_O$ direction, DSO has an out-of-phase tilting of the oxygen octahedra, while the NNO film shows pure in-phase tilting far away from the interface. Fig. 2(c) maps the gradual variations in the ellipticity of the oxygen columns and octahedral tilt angle in NNO as a function of distance from this interface shown in Fig. 2(b). Such precise interface measurements can help set upper bounds in the length scale for templating octahedral rotations of the substrate onto the film [10].

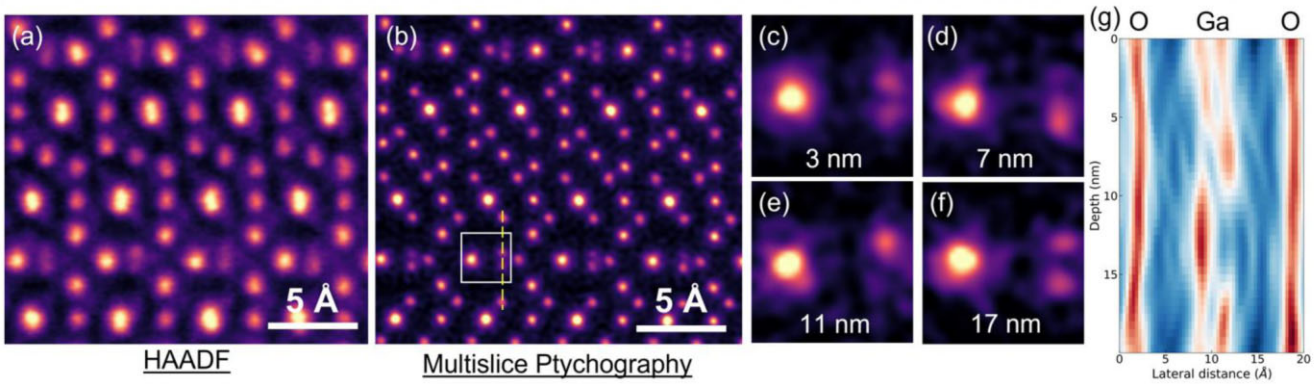

Fig. 1. (a) HAADF image, (b) ptychographic reconstruction of Mg,Zr-doped strontium hexagallate. (c-f) shows slices at different depths of a Sr and Ga site marked with a white box in (b). (g) Depth profile along the yellow line in (b) showing the changing occupancy of the bi-stable Ga site.

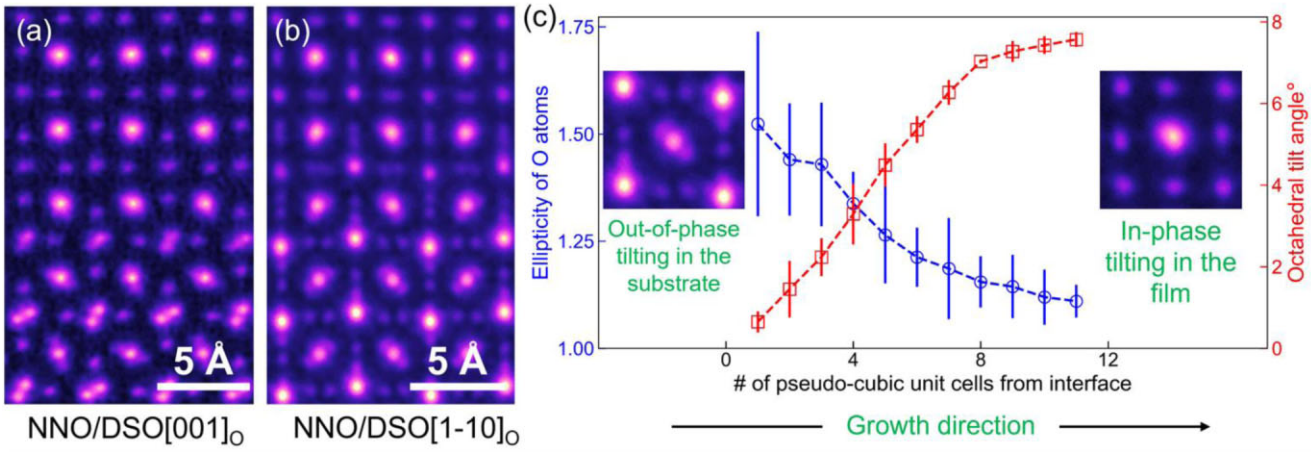

Fig. 2. (a,b) Ptychographic reconstruction of the interface structure of NNO/DSO along two orthogonal directions. (c) Plot of the O column ellipticity and octahedral tilt angle in NNO as a function of distance from the interface shown in (b).

References

1. P Gao *et al.*, *Ultramicroscopy* **184** (2018), p. 177. doi:10.1016/j.ultramic.2017.09.001
2. J Bürger *et al.*, *Ultramicroscopy* **219** (2020), doi:10.1016/j.ultramic.2020.113118
3. MW Tate *et al.*, *Microscopy and Microanalysis* **22** (2016), p. 237, doi:10.1017/S1431927615015664
4. HT Philipp *et al.*, *Microscopy and Microanalysis* **28**(2) (2022), p. 425. doi:10.1017/S1431927622000174
5. Y Jiang *et al.*, *Nature* **559** (2018) p. 343. doi:10.1038/S41586-018-0298-5
6. Z Chen *et al.*, *Nature Nanotechnology* **17** (2022), p. 1165. doi:10.1038/s41565-022-01224-y
7. Z Chen *et al.*, *Science* **372** (2021), p. 826. doi:10.1126/science.abg2533
8. C Guguschev *et al.*, *Crystal Growth & Design* **22** (2022) p. 2557. doi:10.1021/acs.cgd.2c00030
9. HKP, et al., *Microscopy and Microanalysis* **28**(S1) (2022), p. 476. doi:10.1017/S1431927622002574
10. Work supported by the Army Research Office under the ETHOS MURI via cooperative agreement W911NF-21-2-0162 and the AFOSR Hybrid Materials MURI award # FA9550-18-1-0480. Facilities supported by the National Science Foundation (DMR-1719875, DMR-1429155, DMR-2039380, DMR-1719875).